Reseach Article **Open Access**

Liecheng Sun* and Issam E. Harik

Analytical solution to bending of stiffened and continuous antisymmetric laminates

Abstract: Analytical Strip Method is presented for the analysis of the bending-extension coupling problem of stiffened and continuous antisymmetric thin laminates. A system of three equations of equilibrium, governing the general response of antisymmetric laminates, is reduced to a single eighth-order partial differential equation (PDE) in terms of a displacement function. The PDE is then solved in a single series form to determine the displacement response of antisymmetric cross-ply and angle-ply laminates. The solution is applicable to rectangular laminates with two opposite edges simply supported and the other edges being free, clamped, simply supported, isotropic beam supports, or point supports.

Keywords: Analytical solution; Laminates; Plates; Bending-extension coupling; Beams; Point loads

DOI 10.1515/cls-2015-0013
Received January 2, 2015; accepted January 30, 2015

1 Introduction

Stiffened laminated plates in aerospace, marine, and other industrial structures can be optimally and economically designed through proper sizing of the plate and stiffeners. The analysis of stiffened laminated plates is complex and a number of studies dealt with them using numerical methods. Biswal and Ghosh [1] proposed a four-node rectangular element based on the higher order theory for bending analysis of stiffened laminated plates. Kolli and Chandrashekhara [2] developed a finite element model for predicting the global behavior of stiffened laminated plates based on the first order shear deformation theory. Kumar and Mukhopadhyay [3] presented a stiffened plate element for the static and free vibration analyses of laminated stiffened plates. Barik and Mukhopadhyay [4] proposed a stiffened plate element for the static and free vibration stability analysis of arbitrary stiffened plates based on the classical plate theory by neglecting the effect of transverse shear deformation. Harik et al. [5] developed a layer-wise finite element formulation for the bending analysis of stiffened laminated plates. Li and Ren [6] proposed a finite element model to study the bending behavior of stiffened laminated plates based on the higher-order global-local theories. Thinh and Quoc [7] studied free vibration and bending failure of laminated stiffened glass fiber/polyester composite plates with laminated open section and closed section of stiffeners by using finite element method and experiment. Bhar et al. [8] demonstrated the need for using higher-order shear deformation theory instead of first-order shear deformation theory, for obtaining accurate structural response of laminated composite stiffened plates by using finite element method. Li et at. [9] investigated low-velocity impact responses and impact-induced damages evaluation problems for the stiffened composite laminated plates based on the progressive failure model and layerwise/solid-elements method. Hariri et al. [10] studied thin structure with several piezoelectric patches bonded on its surface by using the finite element method. Natarajan et al. [11] studied the static bending and free vibration of cross-ply laminated composite plates using sinusoidal deformation theory which combined isogeometric approach and unified formulation. Mukherjee and Menghani [12] studied aspects of displacements and stresses in laminated composite beams and stiffened plates by using a high-order theory with quadratic isoparametric shape functions. Sadek and Tawfik [13] presented a refined higher-order displacement model for the study of the behavior of concentrically and eccentrically stiffened laminated plates based on C^0 finite element discretization. Qing et al. [14] developed a novel mathematical model for free vibration analysis of stiffened laminated plates by separating consideration of plate and stiffeners based on the semi-analytical solution of the state-vector equation theory. Hadjiloizi et al. [15, 16] analyzed a smart composite piezo-magneto-thermoelastic thin plate with rapidly-varying thickness by using rigorous

***Corresponding Author: Liecheng Sun:** Kentucky Transportation Center, University of Kentucky, Lexington, KY 40506, Unite States, E-mail: charlie.sun@uky.edu., Tel.: +18592577330
Issam E. Harik: Department of Civil Engineering, University of Kentucky, Lexington, KY 40506, Unite States, E-mail: Harik@uky.edu.

three-dimensional formulation as the basis of multiscale asymptotic homogenization. The asymptotic homogenization model is developed using static equilibrium equations and the quasi-static approximation of Maxwell's equations.

The Analytical Strip Method (Harik [17]; Harik and Salamoun [18, 19]) was proposed for the analysis of thin orthotropic and stiffened rectangular plates. Recently, this method was extended to antisymmetric laminates (Sun and Harik [20]).

The objective of this paper is to extend the application of the analytical strip method (hereinafter ASM) to stiffened antisymmetric cross-ply or angle-ply laminated composite plates with bending-extension coupling.

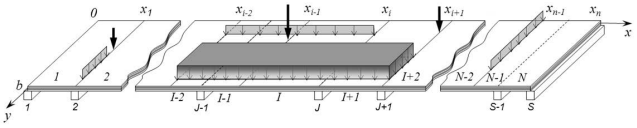

Figure 1: Stiffened plate with strip and edge loadings (Note: The beams are concentric and the lower half of the beams are shown for clarity).

The plates have two parallel edges simply supported and can be subjected to uniform, partial uniform distributed load, patch, line, partial line, and point loads, and to any combination of these loads (Figure 1). The solution procedure requires that the plate be divided into strips whose number depends on the geometric and loading discontinuities. The solution of the governing differential equation of each strip employs the classical method of separation of variables. Unlike the numerical (e.g., Harik, et al. [5]) and semi-numerical methods (Kong and Cheung [21]), the accuracy of the analytic strip method does not depend on the number of strips but on the number of modes considered in the series. Consequently, the number of algebraic equations and the computational difficulties are reduced considerably. The ASM results compared very well with established methods of analysis for isotropic and orthotropic plates (Harik [17]; Harik and Salamoun [18, 19]). Results for stiffened and continuous antisymmetric laminates are not available in the literature. Consequently, the results presented herein are compared with ones derived using the finite element program ANSYS (ANSYS, Inc. [22]).

2 Governing Equations for Antisymmetric Laminated Plate Strips

For plate strip I (Figure 1) in a laminated composite plate, the system of three equations of equilibrium governing the general response can be written as (Whitney and Leissa [23])

$$\begin{bmatrix} L_{11} & L_{12} & L_{13} \\ L_{12} & L_{22} & L_{23} \\ L_{13} & L_{23} & L_{33} \end{bmatrix} \begin{Bmatrix} u_0 \\ v_0 \\ w \end{Bmatrix} = \begin{Bmatrix} 0 \\ 0 \\ q \end{Bmatrix} \tag{1}$$

in which, the displacements in the x, y, and z directions, u_0, v_0, and w, respectively, are presented in terms of the displacement function $\Phi(x, y)$ (Sharma et al. [24])

$$u_0 = (L_{12}L_{23} - L_{13}L_{22})\Phi(x, y) \tag{2a}$$

$$v_0 = (L_{13}L_{21} - L_{23}L_{11})\Phi(x, y) \tag{2b}$$

$$w = (L_{11}L_{22} - L_{12}L_{21})\Phi(x, y) \tag{2c}$$

The differential operators L_{ij} are defined as follows

$$L_{11} = A_{11}\frac{\partial^2}{\partial x^2} + A_{66}\frac{\partial^2}{\partial y^2} \tag{3a}$$

$$L_{12} = (A_{12} + A_{66})\frac{\partial^2}{\partial x \partial y} \tag{3b}$$

$$L_{13} = \\ = -\left[B_{11}\frac{\partial^3}{\partial x^3} + 3B_{16}\frac{\partial^3}{\partial x^2 \partial y} + B_{12}\frac{\partial^3}{\partial x \partial y^2} + B_{26}\frac{\partial^3}{\partial y^3}\right] \tag{3c}$$

$$L_{22} = A_{66}\frac{\partial^2}{\partial x^2} + A_{22}\frac{\partial^2}{\partial y^2} \tag{3d}$$

$$L_{23} = \\ = -\left[B_{16}\frac{\partial^3}{\partial x^3} + B_{12}\frac{\partial^3}{\partial x^2 \partial y} + 3B_{26}\frac{\partial^3}{\partial x \partial y^2} + B_{22}\frac{\partial^3}{\partial y^3}\right] \tag{3e}$$

$$L_{33} = D_{11}\frac{\partial^4}{\partial x^4} + 2(D_{12} + 2D_{66})\frac{\partial^4}{\partial x^2 \partial y^2} + D_{22}\frac{\partial^4}{\partial y^4} \tag{3f}$$

in which A_{ij} are the extensional stiffness coefficients, B_{ij} are the bending-extension coupling stiffness coefficients, and D_{ij} are the bending stiffness coefficients. The stiffness coefficients are given by Reddy [25] and are defined as follows:

$$\left\{A_{ij}, B_{ij}, D_{ij}\right\} = \int_{-\frac{h}{2}}^{\frac{h}{2}} \overline{Q}_{ij}\left\{1, z, z^2\right\} dz; \quad (i, j = 1, 2, 6) \tag{4}$$

where, h is the thickness of the plate, and $\overline{Q}_{ij}$ are reduced stiffness coefficients (Reddy [25]).

For antisymmetric cross-ply laminates, the stiffness coefficients $B_{16} = B_{26} = 0$ and $B_{22} = -B_{11}$ in Eq. 3. For antisymmetric angle-ply laminate, the stiffness coefficients $B_{11} = B_{22} = 0$ in Eq. 3.

The membrane and flexural strains, $\{\varepsilon_0\} = \left\{\varepsilon_{xx}^{(0)}, \varepsilon_{yy}^{(0)}, \gamma_{xy}^{(0)}\right\}^T$ and $\{\kappa\} = \left\{\varepsilon_{xx}^{(1)}, \varepsilon_{yy}^{(1)}, \gamma_{xy}^{(1)}\right\}^T$, respectively, can be presented in terms of the membrane forces, $\{N\} = \{N_x, N_y, N_{xy}\}^T$, and moments, $\{M\} = \{M_x, M_y, M_{xy}\}^T$, as follows

$$\begin{Bmatrix} \{\varepsilon_0\} \\ \{\kappa\} \end{Bmatrix} = \begin{bmatrix} [A] & [B] \\ [B] & [D] \end{bmatrix}^{-1} \begin{Bmatrix} \{N\} \\ \{M\} \end{Bmatrix} \tag{5}$$

where $[A]$, $[B]$, and $[D]$ are the matrices containing A_{ij}, B_{ij}, and D_{ij}, $(i, j = 1, 2, 6)$, respectively. It should be noted that the transverse strains $\{\varepsilon_{xz}, \varepsilon_{yz}, \varepsilon_{zz}\}$ are identically zero in the classical plate theory.

Based on von Kármán's plate theory, the strains in the k^{th} layer can be presented in the following form (Reddy [25])

$$\begin{Bmatrix} \varepsilon_{xx} \\ \varepsilon_{yy} \\ \gamma_{xy} \end{Bmatrix}^k = \begin{Bmatrix} \varepsilon_{xx}^{(0)} \\ \varepsilon_{yy}^{(0)} \\ \gamma_{xy}^{(0)} \end{Bmatrix}^k + z_k \begin{Bmatrix} \varepsilon_{xx}^{(1)} \\ \varepsilon_{yy}^{(1)} \\ \gamma_{xy}^{(1)} \end{Bmatrix}^k \tag{6}$$

in which z_k is the distance between the midplane of the plate and a point in the k^{th} orthotropic lamina.

The linear constitutive relations for the k^{th} orthotropic lamina in the principal material coordinates of the lamina are

$$\begin{Bmatrix} \sigma_{xx} \\ \sigma_{yy} \\ \tau_{xy} \end{Bmatrix}^k = \begin{bmatrix} \overline{Q}_{11} & \overline{Q}_{12} & \overline{Q}_{16} \\ \overline{Q}_{12} & \overline{Q}_{22} & \overline{Q}_{26} \\ \overline{Q}_{16} & \overline{Q}_{26} & \overline{Q}_{66} \end{bmatrix}^k \begin{Bmatrix} \varepsilon_{xx} \\ \varepsilon_{yy} \\ \gamma_{xy} \end{Bmatrix}^k \tag{7}$$

Based on the derivation by Sharma et al. [24], Eq. 1 can be written as

$$\begin{aligned}(L_{11}L_{22}L_{33} - L_{21}L_{12}L_{33} - L_{32}L_{23}L_{11} + L_{31}L_{12}L_{23} + \\ + L_{32}L_{13}L_{21} - L_{31}L_{13}L_{22})\Phi(x, y) = q(x, y)\end{aligned} \tag{8}$$

The governing differential equation for antisymmetric laminated plates can be derived from Eq. 8 by expanding the differential operators L_{ij}

$$\begin{aligned}A_1\frac{\partial^8\Phi}{\partial x^8} + A_3\frac{\partial^8\Phi}{\partial x^6\partial y^2} + A_5\frac{\partial^8\Phi}{\partial x^4\partial y^4} + \\ + A_7\frac{\partial^8\Phi}{\partial x^2\partial y^6} + A_9\frac{\partial^8\Phi}{\partial y^8} = q(x, y)\end{aligned} \tag{9}$$

in which A_i $(i = 1, 3, \ldots, 9)$ are given by Sharma et al. [24].

3 Isotropic Beam Equations

For the l^{th} isotropic beam $(l = 1, 2, \ldots, S)$, located along the line $x = x_l$ $(l = 0, 1, \ldots, S$, the axial rotation about y-axis is assumed to be fully restrained along the edges $y = 0$ and $y = b$. Considering the bending, torsional and warping stresses, the following pair of differential equations can be derived from the equilibrium of the beam element (Salamoun and Harik [26]):

$$Q_b = D_E\left(bK1\frac{d^4W_b}{dy^4}\right) \tag{10}$$

$$T_b = D_E\left(-bK2\frac{d^2\varphi_b}{dy^2} + b^3K3\frac{d^4\varphi_b}{dy^4}\right) \tag{11}$$

in which,

$$K1 = \frac{E_bI_b}{D_Eb}, \tag{12a}$$

$$K2 = \frac{G_bJ_b}{D_Eb}, \tag{12b}$$

$$K3 = \frac{E_bC_w}{D_Eb^3} \tag{12c}$$

$$D_E = \frac{E_1h^3}{12(1 - \nu_{12}\nu_{21})} \tag{13}$$

Q_b and T_b are respectively the lateral load and twisting moment per unit length applied to the beam element located at $x = x_l$ $(l = 0, 1, \ldots, S)$; D_E is the equivalent flexural rigidity of orthotropic plate and is introduced herein for convenience; W_b and φ_b are respectively the deflection and twist angle of the beam; $K1$, $K2$, and $K3$ are dimensionless constants selected for convenience; E_bI_b = flexural rigidity of the beam; G_bJ_b = torsional rigidity of the beam and E_bC_w = warping rigidity of the beam; E_1 is the elastic modulus in the ply direction; h is the total thickness of plate; b is the length along the on y-direction of the plate; ν_{ij} is Poisson's ratio of the transverse strain in the j-direction to the strain in the i-direction, when stressed in i-direction.

4 The Analytical Strip Method

The laminated plate in Figure 1 is divided into plate strips depending on loading and geometric discontinuities. For a rectangular plate strip I, simply supported along two edges parallel to x-axis ($y = 0$ and $y = b$ in Figure 1), the solution to Eq. 9 can be presented in a single series form

$$\Phi_I(x, y) = \sum_n^\infty \varphi_{nI}(x) \cdot \sin(\beta_n y) \tag{14}$$

in which,

$$\beta_n = \frac{n\pi}{b} \tag{15}$$

and b is the length of the plate along the y-axis. Hereinafter, the subscript I, denoting the I^{th} plate strip, will be dropped in the derivation of the solution to Eq. 9 for strip I.

Substitution of Eq. 14 into Eq. 19 leads to

$$\begin{aligned} &A_1\sum_n^\infty \frac{d^8\varphi_n(x)}{dx^8}\sin(\beta_n y) - A_3\sum_n^\infty \frac{d^6\varphi_n(x)}{dx^6}\beta_n^2\sin(\beta_n y) + \\ &+A_5\sum_n^\infty \frac{d^4\varphi_n(x)}{dx^4}\beta_n^4\sin(\beta_n y) - A_7\sum_n^\infty \frac{d^2\varphi_n(x)}{dx^2}\beta_n^6\sin(\beta_n y) + \\ &+A_9\sum_n^\infty \varphi_n(x)\beta_n^8\sin(\beta_n y) = q(x,y) \end{aligned} \tag{16}$$

Multiplying Eq. 16 by $\sin(\beta_m y)$, integrating from $y = 0$ to b, and summing from $m = 1$ to $m = \infty$, Eq. 16 leads to

$$\begin{aligned} &\sum_m^\infty \{\, A_1\left[\int_0^b \sum_n^\infty \tfrac{d^8\varphi_n(x)}{dx^8}\sin(\beta_n y)\sin(\beta_m y)dy\right] + \\ &-A_3\left[\int_0^b \sum_n^\infty \tfrac{d^6\varphi_n(x)}{dx^6}\beta_n^2\sin(\beta_n y)\sin(\beta_m y)dy\right] \\ &+A_5\left[\int_0^b \sum_n^\infty \tfrac{d^4\varphi_n(x)}{dx^4}\beta_n^4\sin(\beta_n y)\sin(\beta_m y)dy\right] + \\ &-A_7\left[\int_0^b \sum_n^\infty \tfrac{d^2\varphi_n(x)}{dx^2}\beta_n^6\sin(\beta_n y)\sin(\beta_m y)dy\right] \\ &+A_9\left[\int_0^b \sum_n^\infty \varphi_n(x)\beta_n^8\sin(\beta_n y)\sin(\beta_m y)dy\right] \,\} = \\ &= \sum_m^\infty \int_0^b q(x,y)\sin(\beta_m y)dy \end{aligned} \tag{17}$$

Since $\int_0^b \sin(\beta_n y)\sin(\beta_m y)dy = \frac{b}{2}$ for $m = n$, and $\int_0^b \sin(\beta_n y)\sin(\beta_m y)dy = 0$ for $m \neq n$, Eq. 17 reduces to

$$\begin{aligned} &\sum_m^\infty [\, A_1\frac{d^8\varphi_m(x)}{dx^8} - A_3\beta_m^2\frac{d^6\varphi_m(x)}{dx^6} + A_5\beta_m^4\frac{d^4\varphi_m(x)}{dx^4} + \\ &-A_7\beta_m^6\frac{d^2\varphi_m(x)}{dx^2} + A_9\beta_m^8\varphi_m(x)\,] = \\ &\sum_m^\infty \frac{2}{b}\int_0^b q(x,y)\sin(\beta_m y)dy \end{aligned} \tag{18}$$

Eq. 18 is an infinite set of ordinary differential equations for $\varphi_m(x)$ ($m = 1, 2, 3 \ldots \infty$). It is a unidirectional and linear 8^{th} order differential equation that can be solved by the superposition of the homogeneous part, $\Phi_H(x, y)$, and the particular part of the equation, $\Phi_P(x, y)$.

$$\Phi(x,y) = \Phi_H(x,y) + \Phi_P(x,y) \tag{19a}$$

or,

$$\begin{aligned} &\sum_m^\infty \varphi_m(x)sin(\beta_m y) = \\ &= \sum_m^\infty \varphi_{Hm}(x)\sin(\beta_m y) + \sum_m^\infty \varphi_{Pm}(x)\sin(\beta_m y) \end{aligned} \tag{19b}$$

Where, $\Phi_H(x,y) = \sum_m^\infty \varphi_{Hm}(x)\sin(\beta_m y)$ is homogeneous solution, and $\Phi_P(x,y) = \sum_m^\infty \varphi_{Pm}(x)\sin(\beta_m y)$ is particular solution.

4.1 Homogeneous Solution

The homogeneous solution for mode m, $\varphi_{Hm}(x)$, is expressed as follows:

$$\varphi_{Hm}(x) = e^{\gamma_m\beta_m x} \tag{20}$$

The characteristic equation of the homogeneous part of Eq. 18 for mode m is

$$A_1\gamma_m^8\beta_m^8 - A_3\gamma_m^6\beta_m^8 + A_5\gamma_m^4\beta_m^8 - A_7\gamma_m^2\beta_m^8 + A_9\beta_m^8 = 0 \tag{21}$$

in which, $\gamma_m\beta_m$ are the characteristic roots. Eq. 21 can be reduced to a quartic equation that can be solved analytically (Editing group of the Manual of Mathematics [27]) leading to the following general expression for the homogeneous solution, $\Phi_H(x, y)$

$$\begin{aligned} \Phi_H(x) = \sum_m^\infty \Bigg\{ &\begin{matrix} [\, C_{1m}\cosh(\gamma_{1m}\beta_m x) + \\ +[\, C_{3m}\cosh(\gamma_{1m}\beta_m x) + \\ +[\, C_{5m}\cosh(\gamma_{3m}\beta_m x) + \\ +[\, C_{7m}\cosh(\gamma_{3m}\beta_m x) + \end{matrix} \quad \cdots \\ \cdots \quad &\begin{matrix} +C_{2m}\sinh(\gamma_{1m}\beta_m x)\,]\cos(\gamma_{2m}\beta_m x) \\ +C_{4m}\sinh(\gamma_{1m}\beta_m x)\,]\sin(\gamma_{2m}\beta_m x) \\ +C_{6m}\sinh(\gamma_{3m}\beta_m x)\,]\cos(\gamma_{4m}\beta_m x) \\ +C_{8m}\sinh(\gamma_{3m}\beta_m x)\,]\sin(\gamma_{4m}\beta_m x) \end{matrix} \Bigg\} \sin(\beta_m y) \end{aligned} \tag{22}$$

The constants C_{dm} ($d = 1, 2, \ldots, 8$) are determined from the boundary conditions at $x = 0$ and $x = x_n = a$ and the continuity conditions at the intermediate edges x_i ($i = 1, 2, 3, \ldots, n-1$, Figure 1).

4.2 Particular Solution

The separation of variables can be applied to present the load $q(x, y)$ in Eq. 18 as follows

$$q(x,y) = q_0 f(x)g(y) \tag{23}$$

in which q_0 is the load amplitude, and $f(x)$ and $g(y)$ are the load distribution functions in the x and y directions, respectively. The right hand side in Eq. 18 takes the following form

$$\begin{aligned} &\sum_m^\infty \left[\frac{2}{b}\int_0^b q(x,y)\sin(\beta_m y)dy\right] = \\ &= \sum_m^\infty \left[\frac{2}{b}\int_0^b q_0 g(x)f(y)\sin(\beta_m y)dy\right] = \sum_m^\infty \left[q_0 f(x)g_{1m}(y)\right] \end{aligned} \tag{24}$$

in which

$$g_{1m} = \frac{2}{b}\int_0^b g(y)\sin(\beta_m y)dy \tag{25}$$

The general expression for the particular solution $\Phi_P(x, y)$ may now be presented as follows:

$$\Phi_P(x, y) = \sum_m^\infty \frac{q_0 f(x) g_{1m}}{A_9 \beta_m^8}\sin(\beta_m y) \tag{26}$$

The particular solutions for most common strip loadings are shown in Table 1.

When strip I is subjected to more than one load (Figure 1), the method of superposition is employed to determine the particular solution.

$$\Phi_P(x, y) = \sum_{j=1}^r \Phi_P^j(x, y) \tag{27}$$

in which r represents the total number of loads applied on strip I.

4.3 Edge Loading Function

When the plate is subjected to line loads in the y direction or to point loads, it is divided into strips in such a way that the loads are applied along the inner or outer edges of the strips (Figure 1). These loads are expressed in a Levy type Fourier series and incorporated in the solution as discontinuities in the shear force. The edge loading functions $\psi_i(y)$ for most common loadings are shown Table 2.

When the edge x_i is subjected to a combination of loads (e.g. $x = x_1$ in Figure 1), the method of superposition is employed to determine the edge loading function:

$$\psi_i(y) = \sum_{l=1}^s \psi_i^l(y) \tag{28}$$

where s represents the total number of edge loadings applied on edge x_i.

4.4 Boundary Conditions

The boundary conditions along the edge $x = 0$ and $x = x_n = a$ are:

Simply supported edge:

$$u = 0, \tag{29a}$$

$$w = 0, \tag{29b}$$

$$N_{xy} = 0, \tag{29c}$$

$$M_x = 0 \tag{29d}$$

Clamped edge,

$$u = 0, \tag{30a}$$

$$v = 0, \tag{30b}$$

$$w = 0, \tag{30c}$$

$$\frac{\partial w}{\partial x} = 0 \tag{30d}$$

Free edge,

$$V_x = \psi, \tag{31a}$$

$$N_x = 0, \tag{31b}$$

$$N_{xy} = 0, \tag{31c}$$

$$M_x = 0 \tag{31d}$$

Beam support,

$$w = W_b, \tag{32a}$$

$$-\frac{\partial w}{\partial x} = \varphi_b, \tag{32b}$$

$$R_x = Q_b + \psi, \tag{32c}$$

$$M_x = T_b \tag{32d}$$

where, V_x is the shear force in the z direction at a distance x; N_x is the membrane normal force in the x direction; N_{xy} is the membrane shear force in y direction; M_x is the bending moment about y-axis; and ψ is the edge loading function.

4.5 Continuity Conditions

The following continuity conditions are imposed along the common edge $x = x_i$ between strips I and I+1.

$$u_I = u_{(I+1)}, \tag{33a}$$

$$v_I = v_{(I+1)}, \tag{33b}$$

Table 1: Particular solution $\Phi_{PI}(x, y)$ for a laminated plate strip I.

Load Case	$\Phi_{PI}(x, y)$
Case 1 - Partial uniform load q_0 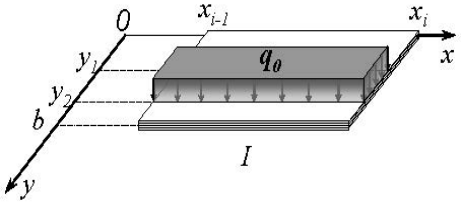	$\Phi_{PI}(x,y) = \frac{2q_0b^8}{A_9\pi^9}\sum_m^\infty \frac{1}{m^9}\left[\cos\left(\frac{m\pi}{b}y_1\right) + -\cos\left(\frac{m\pi}{b}y_2\right)\right]\sin\left(\frac{m\pi}{b}y\right)$
Case 2 – Uniform load q_0 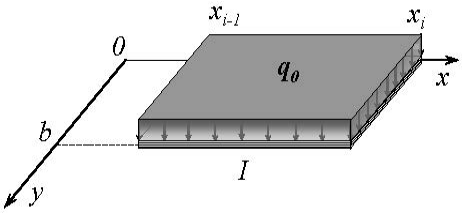	$\Phi_{PI}(x,y) = \frac{4q_0b^8}{A_9\pi^9}\sum_{m=1,3}^\infty \frac{1}{m^9}\sin\left(\frac{m\pi}{b}y\right)$
Case 3 – Line load L_x 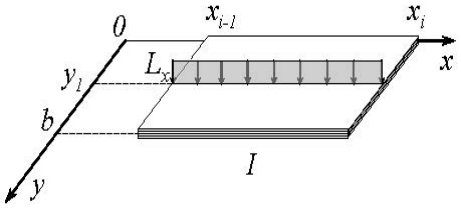	$\Phi_{PI}(x,y) = \frac{2L_xb^7}{A_9\pi^8}\sum_m^\infty \frac{1}{m^8}\sin\left(\frac{m\pi}{b}y_1\right)\cdot\sin\left(\frac{m\pi}{b}y\right)$
Case 4 – Zero load 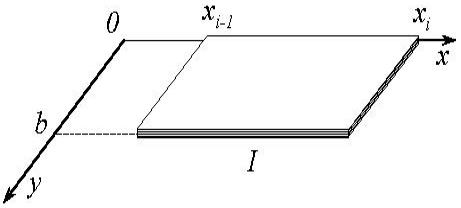	$\Phi_{PI}(x,y) = 0$

$$w_I = w_{(I+1)}, \tag{33c}$$

$$\frac{\partial w_I}{\partial x} = \frac{\partial w_{(I+1)}}{\partial x} \tag{33d}$$

$$M_{xI} = M_{x(I+1)}, \tag{34a}$$

$$N_{xI} = N_{x(I+1)}, \tag{34b}$$

$$V_{xI} = V_{x(I+1)} + \psi_I, \tag{34c}$$

$$N_{xyI} = N_{xy(I+1)} \tag{34d}$$

When a beam is present at $x = x_i$, the following continuity conditions are imposed along the common edge $x = x_i$ between strips I and I+1.

$$u_I = u_{(I+1)}, \tag{35a}$$

$$v_I = v_{(I+1)}, \tag{35b}$$

$$w_I = w_{(I+1)} = w_b, \tag{35c}$$

$$\frac{\partial w_I}{\partial x} = \frac{\partial w_{(I+1)}}{\partial x} = -\varphi_b \tag{35d}$$

$$T_b = M_{x(I+1)} - M_{xI}, \tag{36a}$$

$$N_{xI} = N_{x(I+1)}, \tag{36b}$$

$$Q_b = V_{x(I+1)} - V_{xI} + \psi_I, \tag{36c}$$

Table 2: Edge loading function $\psi_i(y)$ along the edge $x = x_i$.

Load Case	$\psi_i(y)$
Case 1 – Partial line load L_y 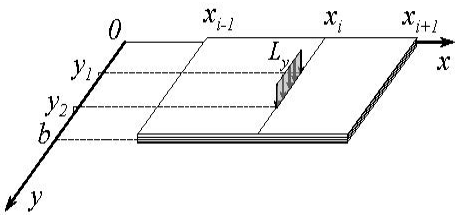	$\psi_i(y) = \frac{2L_y}{\pi}\sum_m^\infty \frac{1}{m}\left[\cos\left(\frac{m\pi}{b}y_1\right) - \cos\left(\frac{m\pi}{b}y_2\right)\right]\sin\left(\frac{m\pi}{b}y\right)$
Case 2 – Line load L_y in y direction 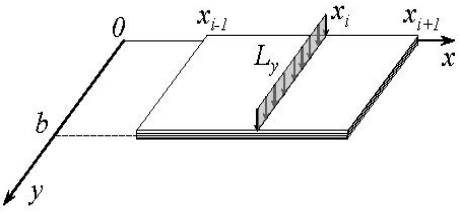	$\psi_i(y) = \frac{4L_y}{\pi}\sum_m^\infty \frac{1}{m}\sin\left(\frac{m\pi}{b}y\right)$
Case 3. – Concentrated load P 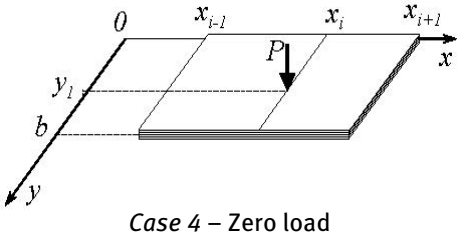	$\psi_i(y) = \frac{2P}{b}\sum_m^\infty \sin\left(\frac{m\pi}{b}y_1\right)\cdot\sin\left(\frac{m\pi}{b}y\right)$
Case 4 – Zero load 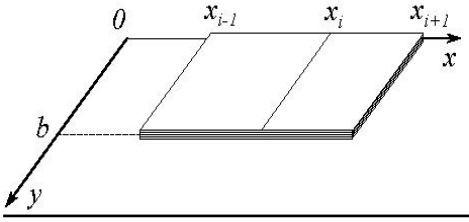	$\psi_i(y) = 0$

$$N_{xyI} = N_{xy(I+1)} \tag{36d}$$

4.6 Solution

A rectangular plate is divided into N-plate strips (Figure 1) depending on the number of loading discontinuities and the locations of the beams and point supports. Eight N-simultaneous equations are generated from the boundary and continuity conditions. For the homogeneous solution of strip I ($I = 1, 2, \ldots, N$), the constants C_{dmI} ($d = 1, 2, \ldots, 8$) are determined for each mode of deflection m ($m = 1, 2, \ldots, \infty$). The particular solution is also determined for each strip I and mode m. The deflection for each strip I is derived by summing the homogeneous and particular solutions. The bending and twisting moments, shears and reactions are then determined from the equations for anti-symmetric cross-ply or angle-ply laminates (Sun [28]).

5 Application

For illustrative purposes the numerical applications deal with different loadings and boundary conditions. All the layers are assumed to be of the same thickness and density and made of the same orthotropic material. The following material parameters are used:

$$E_1 = 132.38\ \text{GPa}(19.2 \times 10^6\text{psi}),$$
$$E_2 = 10.76\ \text{GPa}(1.56 \times 10^6\text{psi}),$$
$$G_{12} = G_{13} = 5.65\ \text{GPa}(0.82 \times 10^6\text{psi}),$$
$$G_{23} = 3.61\ \text{GPa}(0.523 \times 10^6\text{psi}),$$
$$\nu_{12} = 0.24$$

In the following plate bending analysis, uniformly distributed loads, concentrated loads, and patch loads are considered. A simply supported boundary condition is expressed as *S*; clamped as *C*; beam supported as *B*; and free as *F*.

The ASM results are compared with ones derived using the finite element program ANSYS (ANSYS, Inc. [22]) since results for stiffened and continuous antisymmetric laminates are not available in the literature. An eight-node quadrilateral linear layered structural shell element (Shell99) is used to model the laminated plates in ANSYS. This element has both bending and membrane capabilities, and can take up to 250 layers. It can be subjected to in-plane and normal loads. The element has six degrees of freedom at each node.

The numerical results are presented in terms of the dimensionless deflection, $\hat{w}$, and the dimensionless stress, Σ, at the center of plate ($x = a/2$, $y = b/2$), subjected to uniformly distributed or patch load of magnitude q, a line load of magnitude L, or a concentrated load of magnitude P.

$$\hat{w} = \frac{E_2 h^3 \times 10^2}{a^4 q} w - - \quad \text{for a uniform or patch load of magnitude } q \tag{37}$$

$$\hat{w} = \frac{E_2 h^3 \times 10^2}{a^3 L} w - - \text{for a line load of magnitude } L \tag{38}$$

$$\hat{w} = \frac{E_2 h^3 \times 10^2}{a^2 P} w - - \quad \text{for a concentrated load of magnitude } P \tag{39}$$

The dimensionless bending stresses with respect to the x and y axes, Σ_x and Σ_y respectively, and the twisting Σ_{xy} for uniformly distributed or patch loads are

$$\Sigma_x = \frac{h^2}{qa^2}\sigma_x, \tag{40a}$$

$$\Sigma_y = \frac{h^2}{qa^2}\sigma_y, \tag{40b}$$

$$\Sigma_{xy} = \frac{h^2}{qa^2}\sigma_{xy} \tag{40c}$$

For a line load, the non-dimensional stresses are

$$\Sigma_x = \frac{h^2}{La}\sigma_x, \tag{41a}$$

$$\Sigma_y = \frac{h^2}{La}\sigma_y, \tag{41b}$$

$$\Sigma_{xy} = \frac{h^2}{La}\sigma_{xy} \tag{41c}$$

For a concentrated load, the non-dimensional stresses are

$$\Sigma_x = \frac{h^2}{P}\sigma_x, \tag{42a}$$

$$\Sigma_y = \frac{h^2}{P}\sigma_y, \tag{42b}$$

$$\Sigma_{xy} = \frac{h^2}{P}\sigma_{xy} \tag{42c}$$

5.1 Example 1. Edge beam effect on a square antisymmetric angle-ply plate

Uniformly loaded antisymmetric angle-ply square plates, having a width in the x-direction to plate thickness ratio $a/h = 1000$, are studied in this example. h is the plate thickness. The plates are simply supported along the edges at $y = 0$, $y = b$, and $x = 0$, and, beam supported at $x = x_n = a$. Plate with 2 and 10 layers are analyzed, and the ply orientation angle is varied from $\theta = 0^\circ$ to $\theta = 90^\circ$.

The beam, having a square cross section, has a non-dimensional stiffness *K1* (Eq. 12a) that takes the following values: 0.6221 (or beam width = beam depth = $5h$), 1.5, 10, and 30. *K2* and *K3* are calculated using Eqs. 12b and 12c, respectively.

This objective of this example is to show the influence of the edge beam stiffness on the plate behavior. For comparison, results are presented for simply supported and clamped edges at $x = x_n = a$.

Figure 2 shows the dimensionless deflections $\left[\hat{w} = \left(\frac{100E_2h^3}{b^4q}\right)w\right]$ at the center of plate, derived using the ASM (solid lines) and ANSYS (dashed lines). The variation between ASM and ANSYS results is negligible. As the edge beam stiffness increases to *K1* = 30, the plate behaves similar to the one having a clamped edge at $x = a$. For the same boundary conditions, the deflection of the 2-layer plate is larger than that of the 10-layer plate for $0^\circ < \theta < 90^\circ$, and the deflections of the 2-layer and 10-layer plates are equal when $\theta = 0^\circ$ and $\theta = 90^\circ$. This is due to the bending-extension coupling effect, *i.e.*, B_{ij} in Eq. 4 which decreases as the number of layers (n) increases, and approaches zero as n approaches ∞. The larger the number of layers in a laminated plate, having a prescribed thickness, the lesser the effect of the bending-extension coupling. Figure 2 also shows that the bending-extension coupling effect in the two and ten layer laminates is quite pronounced as θ approaches 45°.

Table 3 presents the convergence study of the dimensionless center deflection for a 2-layer and a 10-layer uniformly loaded square laminated plates (30°/-30°/...) for

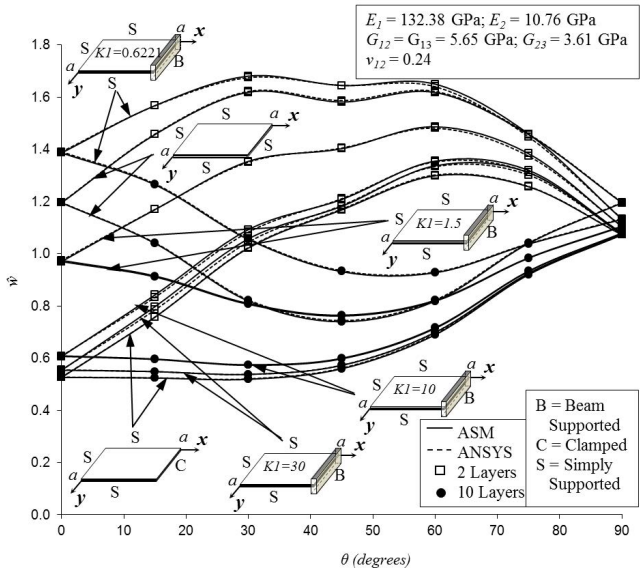

Figure 2: Influence of the beam stiffness, *K1*, and ply orientation angle, θ, on the deflection $\hat{w}\left(\frac{a}{2}, \frac{a}{2}\right) = \left(\frac{100E_2h^3}{a^4q}\right) w$, at the center of a uniformly loaded antisymmetric angle-ply square plate having three edges simply supported and the fourth edge ($x = a$) having varied support conditions.

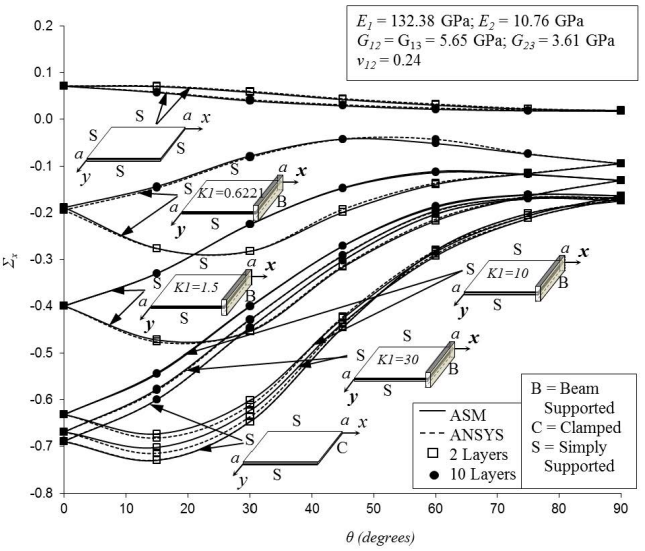

Figure 3: Influence of the beam stiffness, *K1*, and ply orientation angle, θ, on the stress $\Sigma_x\left(0.975a, \frac{a}{2}\right) = \left(\frac{h^2}{qa^2}\right)\sigma_x$

different beam stiffness. The deflection converges rapidly and two significant (or non-zero) terms are sufficient.

Figure 3 presents the variation in the dimensionless stress $\left[\Sigma_x = \left(\frac{h^2}{qb^2}\right)\sigma_x\right]$ at the point $(0.975a, a/2)$ along the plate centerline and in the vicinity of the edge beam. The results derived using ANSYS are drawn in dashed lines and the ones derived using the ASM are drawn in solid lines. The maximum difference between the ANSYS and ASM results is 1.75%, which occurs when *K1* = 30 and $\theta = 15^\circ$ on 2-layer plate. As expected, the stress increases with *K1* and as *K1* approaches 30, the edge supported beam becomes a clamped edge. Table 4 presents the convergence study for the dimensionless stresses at the center of a 2-layer and a 10-layer of uniformly loaded square angle-ply laminated plates (30°/-30°/...). The plates have three simply supported edges and beam support along the edge $x = a$. The results indicate that three significant terms in the series are sufficient for determining the stresses in these plates.

5.2 Example 2. Edge beam effect for a square antisymmetric cross-ply plate

Uniformly loaded antisymmetric cross-ply square plates, having a width in the x-direction to plate thickness ratio $a/h = 1000$, are studied in this example. The plates are simply supported along the edges at $y = 0$, $y = b$, and $x = 0$, and, beam supported at $x = x_n = a$. Plates with 2, 4, 6, 8 and 10 layers are analyzed. The objective of this example is to determine the edge beam effect on a cross ply laminated plate by varying the beam stiffness, *K1* (*K1* = 0.6221, 1.5, 10, and 30). *K1* = 0.6221 represents the case when the beam has a square cross section of width equal to five times the plate thickness, h.

Table 5 presents the deflection and stress, $\hat{w} = \left(\frac{100E_2h^3}{a^4q}\right) w$ and $\Sigma_x = \left(\frac{h^2}{qb^2}\right)\sigma_x$ at the center of plate. The ASM results are compared with ones derived using ANSYS and the difference between the two is negligible. The deflection and stress for the 2-layer plate are always greater than the ones for the 10-layer for the same edge beam stiffness, *K1*. This is due to the bending-extension coupling effect, i.e., B_{ij} in Eq. 4 decreases as the number of layers (n) increases, and approaches zero as n approaches ∞. The larger the number of layers in a laminated plate, having a prescribed thickness, the lesser is the effect of the bending-extension coupling. As the number of layers increases, for the same plate thickness, the magnitudes of the deflection and stress decreases. For example, the deflection at the center of the plate for *K1* = 0.6221 and $n = 2$ is $\hat{w} = 1.9262$, while for four layers $\hat{w} = 1.2958$, a decrease in the magnitude of the deflection of 32.7%. For the 8-layer plate, $\hat{w} = 1.2037$, while for the 10-layer plate $\hat{w} = 1.1936$, a decrease of 0.8%. This is a clear indication of the reduction of the influence of the effect of the bending-extension coupling. Similar deduction can be made for the stresses.

Table 6 presents the convergence study on the dimensionless center deflection and stresses of 2-layer, 4-layer and 8-layer uniformly loaded antisymmetric cross-ply square plates, with three different boundary beams

Table 3: ASM convergence study for the center deflection, $\hat{w}(a/2, a/2)^1$ of an antisymmetric angle-ply square plate (30°/-30°/30°/-30°/...) having three edges simply supported and the fourth edge ($x = a$) having a beam support of different non-dimensional stiffness *K1* (a/h = 1000, E_1 = 132.38 GPa, E_2 = 10.76 GPa, $G_{12} = G_{13}$ = 5.65 GPa, G_{23} = 3.61 GPa, ν_{12} = 0.24).

n^2	m^3	$\hat{w}^1$			
		K1[4] = 0.6221	*K1* = 1.5	*K1* = 10	*K1* = 30
2	1	1.71286	1.38606	1.12445	1.08903
	3	−0.03510	−0.03486	−0.03472	−0.03469
	5	0.00351	0.00350	0.00350	0.00350
	7	−0.00069	−0.00069	−0.00068	−0.00069
	9	0.00020	0.00020	0.00020	0.00020
	$\sum_{m=1,3}^{9}$	1.68078	1.35421	1.09275	1.05735
10	1	1.07414	0.82507	0.59161	0.55645
	3	−0.02152	−0.02115	−0.02091	−0.02089
	5	0.00241	0.00240	0.00240	0.00241
	7	−0.00050	−0.00049	−0.00049	−0.00050
	9	0.00015	0.00014	0.00014	0.00015
	$\sum_{m=1,3}^{9}$	1.05468	0.80597	0.57275	0.53762

[1] $\hat{w}\left(\frac{a}{2}, \frac{a}{2}\right) = \left(\frac{100E_2h^3}{a^4q}\right) w$

[2] n = number of layers

[3] m = mode of deflection

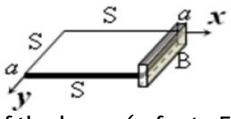

[4] *K1* = dimensionless flexural rigidity of the beam (refer to Eq. 12a). *K2* and *K3* are derived using Eqs. 12b and 12c, respectively. (*K1* = 0.6221 refers to beam width = beam depth = 5h)

Table 4: Effect of the beam stiffness, *K1*, on the convergence of stresses $\Sigma(a/2, a/2) = (h^2/qa^2)\sigma$ at the center of an antisymmetric angle-ply square plate (30°/-30°/30°/-30°/...) having three edges simply supported and the fourth edge ($x = a$) beam supported (a/h = 1000, E_1 = 132.38 GPa, E_2 = 10.76 GPa, $G_{12} = G_{13}$ = 5.65 GPa, G_{23} = 3.61 GPa, ν_{12} = 0.24).

n^1	m^2	*K1*[3]											
		0.6221			1.5			10			30		
		Σ_x	Σ_y	Σ_{xy}	Σ_x	Σ_y	Σ_{xy}	Σ_x	Σ_y	Σ_{xy}	Σ_x	Σ_y	Σ_{xy}
2	1	0.4528	0.2207	0.1863	0.4254	0.1951	0.1743	0.4007	0.1739	0.1635	0.3972	0.1710	0.1619
	3	−0.0262	−0.0246	−0.0116	−0.0262	−0.0245	−0.0116	−0.0262	−0.0244	−0.0115	−0.0262	−0.0244	−0.0115
	5	0.0059	0.0065	0.0028	0.0059	0.0065	0.0028	0.0059	0.0065	0.0028	0.0059	0.0065	0.0028
	7	−0.0023	−0.0025	−0.0011	−0.0023	−0.0025	−0.0011	−0.0023	−0.0025	−0.0011	−0.0023	−0.0025	−0.0011
	9	0.0011	0.0012	0.0005	0.0011	0.0012	0.0005	0.0011	0.0012	0.0005	0.0011	0.0012	0.0005
	$\sum_{m=1,3}^{9}$	0.4313	0.2012	0.1769	0.4040	0.1758	0.1649	0.3793	0.1546	0.1541	0.3758	0.1517	0.1526
10	1	0.3456	0.1633	0.1720	0.3154	0.1403	0.1556	0.2816	0.1172	0.1377	0.2762	0.1136	0.1348
	3	−0.0256	−0.0185	−0.0137	−0.0254	−0.0182	−0.0136	−0.0252	−0.0181	−0.0135	−0.0252	−0.0181	−0.0135
	5	0.0066	0.0053	0.0036	0.0066	0.0053	0.0036	0.0066	0.0053	0.0036	0.0066	0.0053	0.0036
	7	−0.0025	−0.0021	−0.0014	−0.0025	−0.0021	−0.0014	−0.0025	−0.0021	−0.0014	−0.0025	−0.0021	−0.0014
	9	0.0012	0.0010	0.0007	0.0012	0.0010	0.0007	0.0012	0.0010	0.0007	0.0012	0.0010	0.0007
	$\sum_{m=1,3}^{9}$	0.3253	0.1490	0.1612	0.2953	0.1263	0.1449	0.2616	0.1033	0.1271	0.2562	0.0998	0.1242

[1] n = number of layers

[2] m = mode of deflection

[3] *K1* = dimensionless flexural rigidity of the beam (refer to Eq. 12a). *K2* and *K3* are derived using Eqs. 12b and 12c, respectively. (*K1* = 0.6221 refers to beam width = beam depth = 5h)

at $x = a$. It is clear that for any beam stiffness, both sufficiently converged deflection and stress results on x-direction can be obtained as series item m up to 5. It is obvious that the convergence rate of Σ_y is slower than convergence rate of Σ_x. It is sufficiently converged on Σ_y when series item m up to 9.

5.3 Example 3. Rectangular antisymmetric angle-ply plate having two interior beams

Uniformly-loaded antisymmetric angle-ply rectangular plates, having a width in the y-direction to plate thickness ratio b/h = 1000 and an aspect ratio a/b = 2 (a = *plate*

Table 5: Effect of beam stiffness (*K1*) and number of layers (n) on the deflection $\hat{w}^1$ and stresses Σ_x^1 at the center of uniformly loaded anti-symmetric cross-ply square laminates having three edges simply supported and the fourth edge ($x = a$) beam supported (a/h = 1000, E_1 = 132.38 GPa, E_2 = 10.76 GPa, $G_{12} = G_{13}$ = 5.65 GPa, G_{23} = 3.61 GPa, ν_{12} = 0.24).

		K1[5]							
n	Method	0.6221		1.5		10		30	
		$\hat{w}$	Σ_x	$\hat{w}$	Σ_x	$\hat{w}$	Σ_x	$\hat{w}$	Σ_x
	ASM[2]	1.9262	0.1295	1.6579	0.1285	1.4410	0.1270	1.4116	0.1267
2	ANSYS[3]	1.9110	0.1294	1.6500	0.1278	1.4310	0.1258	1.4000	0.1254
	% Diff.[4]	0.79	0.11	0.47	0.51	0.69	0.92	0.82	1.06
	ASM	1.2958	0.0709	1.0856	0.0696	0.8823	0.0675	0.8518	0.0671
4	ANSYS	1.2940	0.0715	1.0860	0.0700	0.8820	0.0676	0.8513	0.0671
	% Diff.	0.14	−0.79	−0.04	−0.50	0.03	−0.16	0.06	−0.08
	ASM	1.2261	0.0640	1.0250	0.0626	0.8248	0.0603	0.7943	0.0599
6	ANSYS	1.2250	0.0645	1.0260	0.0629	0.8251	0.0605	0.7944	0.0600
	% Diff.	0.09	−0.75	−0.10	−0.53	−0.04	−0.26	−0.01	−0.19
	ASM	1.2037	0.0615	1.0056	0.0601	0.8065	0.0577	0.7760	0.0573
8	ANSYS	1.2030	0.0619	1.0070	0.0603	0.8070	0.0578	0.7763	0.0574
	% Diff.	0.06	−0.62	−0.14	−0.46	−0.06	−0.22	−0.04	−0.16
	ASM	1.1936	0.0603	0.9969	0.0588	0.7983	0.0564	0.7679	0.0559
10	ANSYS	1.1940	0.0606	0.9981	0.0590	0.7989	0.0565	0.7682	0.0560
	% Diff.	−0.03	−0.57	−0.12	−0.43	−0.07	−0.22	−0.05	−0.17

[1] $\hat{w} = \left(\frac{100E_2h^3}{a^4q}\right) w$; $\Sigma_x = \left(\frac{h^2}{a^2q}\right) \sigma_x$

[2] ASM = Analytical Strip Method

[3] ANSYS = Finite Element Analysis program (ANSYS Inc., 2007)

[4] % Diff. = percent difference: $\left(100\frac{\hat{w}_{ANSYS}-\hat{w}_{ASM}}{\hat{w}_{ASM}}\right)$ or $\left(100\frac{\Sigma_{ANSYS}-\Sigma_{ASM}}{\Sigma_{ASM}}\right)$

[5] *K1* = dimensionless flexural rigidity of the beam (refer to Eq. 12a).
K2 and *K3* are derived using Eqs. 12b and 12c, respectively.
(*K1* = 0.6221 refers to beam width = beam depth = 5h)

length in x-direction), are studied in this example. The plate is simply supported along the edge $y = 0$ and $y = b$, and free along the edges on $x = 0$ and $x = a = 2b$. Two intermediate beams parallel to the y-axis, support the inside plate at $x = 0.25a$, and $x = 0.925a$. The beams have the same stiffness, *K1* = 1.5 (Eq. 12a). The objective of this example is to study the effect of the ply-orientation angle and the number of layers on the deflections and stresses in this plate.

Figure 4 shows the uniformly loaded laminated 10-layer $(-45/45)_5$ plate and its support conditions along with the contour of dimensionless deflection, $\hat{w} = \left(\frac{100E_2h^3}{b^4q}\right) w$ derived using ASM. Table 7 presents the ANSYS and the ASM dimensionless deflections at different locations in the plate and the effect of the ply angle and number of layers on the dimensionless deflections at different locations in the plate. The maximum difference between the ANSYS and ASM results is 1.664% which occurs when $\theta = 30^\circ$ in a 2-layer plate at the center of the free edge at $x = a$. The difference at points away from the free edge at $x = a$ is less than 1%.

Table 8 presents the effect of ply angle and number of layers on the laminate's dimensionless stresses $\Sigma_x = \left(\frac{h^2}{b^2q}\right) \sigma_x$, $\Sigma_y = \left(\frac{h^2}{b^2q}\right) \sigma_y$, and $\Sigma_{xy} = \left(\frac{h^2}{b^2q}\right) \sigma_{xy}$, at the mid-span of beam 1 ($x = a/4$, $y = b/2$ in Figure 4), center of the laminate ($x = a/2$, $y = b/2$), and the mid-span of beam 2 ($x = 0.925a$, $y = b/2$). The maximum stress difference between ANSYS and ASM is 4.88% and that occurs at the center of 2-layer laminate when ply angle $\theta = 60^\circ$ for Σ_{xy}. This difference comes from ANSYS boundary condition on beam warping restriction. Due to the limitation from ANSYS, when beam warping is limited, the laminate at points corresponding to beam are limited as well. The majority of the differences in the results between ANSYS and ASM are smaller than 3.0% (Table 8). At the center of the plate, Σ_x decreases from a maximum value of $\Sigma_x = 0.4122$ at $\theta = 0^\circ$ to a minimum value of $\Sigma_x = 0.0396$ at $\theta = 90^\circ$, for both 2-layer and 10-layer plates. On the other hand, Σ_y increases

Table 6: Influence of the number of layers on the ASM convergence of the center deflection ($\hat{w}^1$) and stresses (Σ_x^1 and Σ_y^1) of antisymmetric cross-ply square plates having three edges simply supported and the fourth edge ($x = a$) beam supported (a/h = 1000, E_1 = 132.38 GPa, E_2 = 10.76 GPa, $G_{12} = G_{13}$ = 5.65 GPa, G_{23} = 3.61 GPa, ν_{12} = 0.24).

n^2	m^3	$K1^4$								
		0.6221			1.5			10		
		$\hat{w}$	Σ_x	Σ_y	$\hat{w}$	Σ_x	Σ_y	$\hat{w}$	Σ_x	Σ_y
2	1	1.9461	0.1311	0.6993	1.6778	0.1300	0.6053	1.4609	0.1286	0.5293
	3	−0.0213	−0.0018	−0.0675	−0.0213	−0.0019	−0.0675	−0.0213	−0.0019	−0.0675
	5	0.0016	0.0003	0.0145	0.0017	0.0003	0.0145	0.0017	0.0003	0.0145
	7	−0.0003	−0.0001	−0.0052	−0.0003	−0.0001	−0.0052	−0.0003	−0.0001	−0.0052
	9	0.0001	0.0001	0.0024	0.0001	0.0001	0.0024	0.0001	0.0001	0.0024
	$\sum_{m=1,3}^{9}$	1.9262	0.1295	0.6434	1.6579	0.1285	0.5495	1.4410	0.1270	0.4734
4	1	1.3067	0.0719	0.6387	1.0964	0.0706	0.5378	0.8932	0.0685	0.4401
	3	-0.0116	-0.0012	-0.0503	-0.0116	-0.0012	-0.0504	-0.0116	-0.0012	-0.0504
	5	0.0009	0.0002	0.0105	0.0009	0.0002	0.0105	0.0009	0.0002	0.0105
	7	−0.0002	−0.0001	−0.0038	−0.0002	−0.0001	−0.0038	−0.0002	−0.0001	−0.0038
	9	0.0001	0.0000	0.0018	0.0001	0.0000	0.0018	0.0000	0.0000	0.0018
	$\sum_{m=1,3}^{9}$	1.2958	0.0709	0.5968	1.0856	0.0696	0.4959	0.8823	0.0675	0.3982
8	1	1.2135	0.0625	0.6719	1.0154	0.0610	0.5641	0.8163	0.0587	0.4555
	3	−0.0104	−0.0011	−0.0512	−0.0104	−0.0012	−0.0513	−0.0105	−0.0012	−0.0513
	5	0.0008	0.0002	0.0106	0.0008	0.0002	0.0106	0.0008	0.0002	0.0106
	7	−0.0001	−0.0001	−0.0039	−0.0001	−0.0001	−0.0039	−0.0001	−0.0001	−0.0039
	9	0.0000	0.0000	0.0018	0.0000	0.0000	0.0018	0.0000	0.0000	0.0018
	$\sum_{m=1,3}^{9}$	1.2037	0.0615	0.6293	1.0056	0.0601	0.5214	0.8065	0.0577	0.4127

[1] $\hat{w} = \left(\frac{100E_2h^3}{a^4q}\right) w$; $\Sigma = \left(\frac{h^2}{a^2q}\right) \sigma$

[2] n = number of layers

[3] m = mode of deflection

[4] *K1* = dimensionless flexural rigidity of the beam.).

K2 and *K3* are derived using Eqs. 12b and 12c, respectively.

(*K1* = 0.6221 refers to beam width = beam depth = 5h)

from a minimum value of Σ_y = 0.0758 at $\theta = 0^\circ$ to maximum value of Σ_y = 0.7162 at $\theta = 90^\circ$, for both 2-layer and 10-layer plates. Shear stresses Σ_{xy} have similar values for 2-layer and 10-layer plates, are close to zero at points $\theta = 0^\circ$ and $\theta = 90^\circ$, and reach maximum values when $\theta = 60^\circ$. The stresses on two beam positions have similar trends.

5.4 Example 4. Antisymmetric angle-ply plate having two internal point supports

The ASM can be applied to a laminated plate having internal point supports. A uniformly-loaded antisymmetric angle-ply rectangular plate, having a width in the y-direction to plate thickness ratio b/h = 1000 and an aspect ratio a/b =2 (a and b are the dimensions of plate in the x and y directions, respectively), is studied in this example. The plate is simply supported along the edges $y = 0$ and $y = b$, and free along the edges $x = 0$ and $x = a$ =2b. Two internal point supports are located at $x = 0.4b$, $y = b/2$ and $x = 1.7b$, $y = b/2$, respectively.

The plate is divided into strips in such a way that the point supports are located along the common edge between two strips. The solution to this problem is achieved by applying the flexibility (or force) method which involved releasing the deflections at the point supports and generating the flexibility matrix to determine the reactions at the supports that are required to cancel these deflections. Figure 5 shows the loading and support conditions for the plate, and displays the contour of dimensionless deflection $\left[\hat{w} = \left(\frac{100E_2h^3}{b^4q}\right) w\right]$, derived using the ASM for a 2-layer (-45/45) rectangular laminated plate.

Figure 6 shows the variation of the dimensionless deflections, $\hat{w}$, with the ply angle θ, at the following three

Table 7: Effect of ply angle, θ and number of layers, n, on the deflection $\hat{w}^1$ of a uniformly loaded rectangular antisymmetric angle-ply plate (a/b = 2, $\theta^\circ/-\theta^\circ/\theta^\circ/\ldots/-\theta^\circ$) with two internal beam supports (Fig. 4) (b/h = 1000, E_1 = 132.38 GPa, E_2 = 10.76 GPa, G_{12} = G_{13} = 5.65 GPa, G_{23} = 3.61 GPa, ν_{12} = 0.24).

θ°	n	Method	$\hat{w}^5_{Left}$	$\hat{w}^6_{Beam1}$	$\hat{w}^7_{Center}$	$\hat{w}^8_{Beam2}$	$\hat{w}^9_{Right}$
0°	2	ASM[2]	1.5526	0.9280	1.7092	0.6648	0.4768
		ANSYS[3]	1.5475	0.9288	1.7160	0.6647	0.4711
		% Diff.[4]	0.327	−0.085	−0.395	0.008	1.206
	10	ASM	1.5526	0.9280	1.7092	0.6648	0.4768
		ANSYS	1.5475	0.9288	1.7160	0.6647	0.4711
		% Diff.	0.327	−0.085	−0.395	0.008	1.206
30°	2	ASM	2.1361	0.8821	2.2322	0.6423	0.5459
		ANSYS	2.1380	0.8827	2.2360	0.6430	0.5370
		% Diff.	−0.089	−0.062	−0.169	−0.107	1.664
	10	ASM	1.6263	0.8743	1.5267	0.6380	0.5656
		ANSYS	1.6220	0.8748	1.5290	0.6377	0.5573
		% Diff.	0.266	−0.057	−0.148	0.054	1.493
45°	2	ASM	2.2034	0.8107	2.2366	0.5945	0.5641
		ANSYS	2.2070	0.8111	2.2420	0.5947	0.5576
		% Diff.	−0.163	−0.045	−0.241	−0.041	1.170
	10	ASM	1.5177	0.7518	1.3600	0.5624	0.5569
		ANSYS	1.5220	0.7524	1.3630	0.5623	0.5518
		% Diff.	−0.285	−0.073	−0.220	0.017	0.926
60°	2	ASM	2.1750	0.6818	2.1453	0.5110	0.5244
		ANSYS	2.1650	0.6801	2.1320	0.5094	0.5181
		% Diff.	0.460	0.243	0.621	0.310	1.224
	10	ASM	1.3698	0.5815	1.2269	0.4489	0.4824
		ANSYS	1.3680	0.5802	1.2210	0.4476	0.4784
		% Diff.	0.134	0.223	0.483	0.283	0.839
90°	2	ASM	1.2648	0.3514	1.1640	0.2941	0.3289
		ANSYS	1.2630	0.3512	1.1610	0.2939	0.3244
		% Diff.	0.139	0.044	0.258	0.065	1.402
	10	ASM	1.2648	0.3514	1.1640	0.2941	0.3289
		ANSYS	1.2630	0.3512	1.1610	0.2939	0.3244
		% Diff.	0.139	0.044	0.258	0.065	1.402

[1] $\hat{w} = \left(\frac{100E_2h^3}{a^4q}\right) w$

[2] ASM = Analytical Strip Methed

[3] ANSYS = Finite Element Analysis program (ANSYS Inc., 2007)

[4] % Diff. = percent difference = $100\left(\frac{\hat{w}_{ANSYS}-\hat{w}_{ASM}}{\hat{w}_{ASM}}\right)$

[5] $\hat{w}_{Left} = \hat{w}$ at $x = 0$ and $y = b/2$

[6] $\hat{w}_{Beam1} = \hat{w}$ at $x = a/4$ (beam 1 position) and $y = b/2$

[7] $\hat{w}_{Center} = \hat{w}$ at $x = a/2$ and $y = b/2$

[8] $\hat{w}_{Beam2} = \hat{w}$ at $x = 0.925a$ (beam 2 position) and $y = b/2$

[9] $\hat{w}_{Right} = \hat{w}$ at $x = a$ and $y = b/2$

points in the plate: ($x = 0$, $y = b/2$), ($x = a/2$, $y = b/2$), and ($x = a$, $y = b/2$). Results derived using the ASM and ANSYS are presented for a 2 and 10 layer plate. The results are in very good agreement. It is interesting to note the variation in $\hat{w}$ with θ. At the center of the plate ($x = a/2$, $y = b/2$), the deflection for the 2-layer plate is larger than that of the 10-layer plate for $0^\circ < \theta < 90^\circ$. At the center of the free edges ($x = 0$, $y = b/2$ and $x = a$, $y = b/2$), the de-

Table 8: Effect of ply angle, θ and number of layers, n, on the stress Σ^1 at the center of the plate and beams of a uniformly loaded rectangular antisymmetric angle-ply plate (a/b = 2, $\theta^\circ/-\theta^\circ/\theta^\circ/\ldots/-\theta^\circ$) with two internal beam supports (Fig. 4) (b/h = 1000, E_1 = 132.38 GPa, E_2 = 10.76 GPa, $G_{12} = G_{13}$ = 5.65 GPa, G_{23} = 3.61 GPa, ν_{12} = 0.24).

θ°	n	Method	Middle of Beam 1			Center of Plate			Middle of Beam 2		
			Σ_x	Σ_y	Σ_{xy}	Σ_x	Σ_y	Σ_{xy}	Σ_x	Σ_y	Σ_{xy}
0°	2	ASM[2]	−0.7757	0.0297	0.0000	0.4122	0.0758	0.0000	−0.6537	0.0193	0.0000
		ANSYS[3]	−0.7775	0.0296	0.0000	0.4140	0.0769	0.0000	−0.6524	0.0191	0.0000
		% Diff.[4]	−0.226	0.543	0.009	−0.446	−1.465	0.063	0.199	0.908	0.001
	10	ASM	−0.7757	0.0297	0.0000	0.4122	0.0758	0.0000	−0.6537	0.0193	0.0000
		ANSYS	−0.7775	0.0296	0.0000	0.4140	0.0769	0.0000	−0.6524	0.0191	0.0000
		% Diff.	−0.226	0.543	0.009	−0.446	−1.465	0.063	0.199	0.908	0.001
30°	2	ASM	−0.6517	−0.1326	−0.2438	0.4110	0.2209	0.1733	−0.6230	−0.1362	−0.2279
		ANSYS	−0.6552	−0.1334	−0.2452	0.4166	0.2263	0.1762	−0.6265	−0.1373	−0.2307
		% Diff.	−0.531	−0.590	−0.573	−1.371	−2.423	−1.679	−0.559	−0.841	−1.218
	10	ASM	−0.3855	−0.0668	−0.1728	0.3325	0.1769	0.1690	−0.3754	−0.0767	−0.1697
		ANSYS	−0.3849	−0.0667	−0.1725	0.3315	0.1757	0.1684	−0.3731	−0.0762	−0.1687
		% Diff.	0.146	0.148	0.172	0.298	0.667	0.336	0.623	0.672	0.610
45°	2	ASM	−0.3979	−0.1797	−0.1866	0.3174	0.3660	0.2207	−0.4112	−0.2055	−0.1989
		ANSYS	−0.3995	−0.1805	−0.1874	0.3216	0.3724	0.2240	−0.4109	−0.2049	−0.1981
		% Diff.	−0.404	−0.452	−0.451	−1.317	−1.751	−1.487	0.062	0.310	0.381
	10	ASM	−0.1861	−0.0683	−0.1013	0.2534	0.2934	0.2176	−0.2114	−0.1031	−0.1251
		ANSYS	−0.1872	−0.0689	−0.1019	0.2570	0.2982	0.2209	−0.2115	−0.1030	−0.1251
		% Diff.	−0.576	−0.757	−0.605	−1.405	−1.620	−1.504	−0.054	0.080	0.038
60°	2	ASM	−0.2473	−0.0969	−0.0665	0.2234	0.5907	0.2326	−0.2637	−0.1439	−0.0852
		ANSYS	−0.2396	−0.0940	−0.0636	0.2150	0.5702	0.2213	−0.2544	−0.1412	−0.0825
		% Diff.	3.119	2.962	4.415	3.749	3.469	4.877	3.528	1.906	3.212
	10	ASM	−0.1120	−0.0029	−0.0200	0.1649	0.4696	0.2238	−0.1315	−0.0558	−0.0455
		ANSYS	−0.1082	−0.0028	−0.0195	0.1586	0.4482	0.2139	−0.1270	−0.0546	−0.0443
		% Diff.	3.377	1.433	2.607	3.841	4.551	4.438	3.420	2.101	2.506
90°	2	ASM	−0.1216	0.1841	0.0000	0.0396	0.7162	0.0000	−0.1244	0.1487	0.0000
		ANSYS	−0.1187	0.1795	0.0000	0.0395	0.6926	0.0000	−0.1213	0.1442	0.0000
		% Diff.	2.357	2.521	0.002	0.501	3.296	0.001	2.467	3.028	0.003
	10	ASM	−0.1216	0.1841	0.0000	0.0396	0.7162	0.0000	−0.1244	0.1487	0.0000
		ANSYS	−0.1187	0.1795	0.0000	0.0395	0.6926	0.0000	−0.1213	0.1442	0.0000
		% Diff.	2.357	2.521	0.002	0.501	3.296	0.001	2.467	3.028	0.003

[1] $\Sigma = \left(\frac{h^2}{a^2 q}\right)\sigma$

[2] ASM = Analytical Strip Methed

[3] ANSYS = Finite Element Analysis program (ANSYS Inc., 2007)

[4] % Diff. = percent difference: $\left(100\frac{\Sigma_{ANSYS}-\Sigma_{ASM}}{\Sigma_{ASM}}\right)$

flection for the 2-layer plate is smaller than that of the 10-layer plate for the range of $0^\circ < \theta < 20^\circ$ and $0^\circ < \theta < 40^\circ$, respectively. Figure 7 presents the dimensionless stresses $\left[\Sigma_x = \left(\frac{h^2}{b^2 q}\right)\sigma_x, \Sigma_y = \left(\frac{h^2}{b^2 q}\right)\sigma_y, \text{ and } \Sigma_{xy} = \left(\frac{h^2}{b^2 q}\right)\sigma_{xy}\right]$ at the center of the plate, ($x = a/2$, $y = b/2$) derived using ASM and ANSYS.

5.5 Example 5. Antisymmetric angle-ply 6-layer square laminated plate having two beam supports, subjected to a patch load and a concentrated load

This example deals with an antisymmetric angle-ply 6-layer square laminated plate (-15/-45/-75/75/45/15) sub-

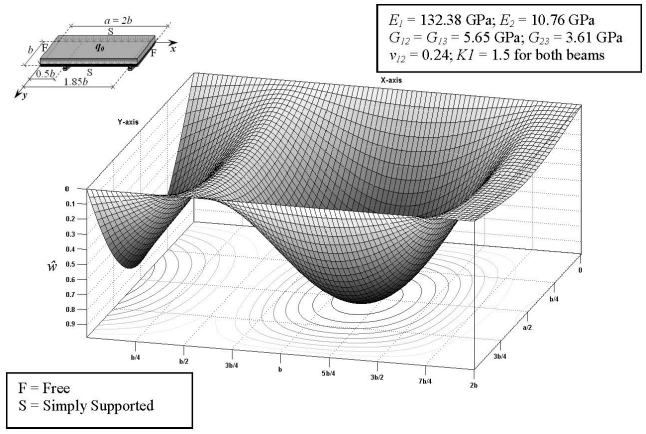

Figure 4: Contour of the dimensionless deflection, $\hat{w} = \left(\frac{100E_2h^3}{b^4q}\right) w$, for a uniformly loaded antisymmetric angle-ply 10-layer $(-45/45)_5$ rectangular laminated plate (Note: the isotropic beams are concentric and only half of the beams on bottom side of the plate are shown for clarity).

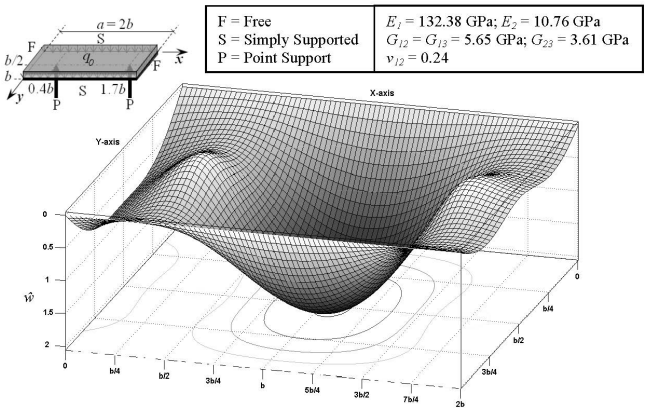

Figure 5: Contour of the dimensionless deflection, $\hat{w} = \left(\frac{100E_2h^3}{b^4q}\right) w$, for a uniformly loaded antisymmetric angle-ply 2-layer (-45/45) rectangular laminated plate $(a/b = 2)$ having simply supported on $y = 0$ and $y = b$, two point supports at $x = 0.4b$, $y = b/2$ and $x = 1.7b$, $y = b/2$, and free at $x = 0$ and $x = 2b$.

jected to a patch load ($a/10 \le x \le a/2$, $a/10 \le y \le a/2$) and a concentrated load ($x = 37a/40$, $y = 3a/4$). The plate has the following support conditions: simple support along the edges $y = 0$ and $y = b$, beam support ($K1 = 1.5$) along the edge $x = 0$, free support along the edge $x =$ a, intermediate beam support ($K1 = 10$) parallel to the y-axis at $x = 7a/8$ (Figure 8).

The objective of this example is to show that the ASM is capable of dealing with laminated plates having complex boundary, support, and loading conditions.

Figure 8 presents the contour of the dimensionless deflection $\hat{w}$ generated using the ASM. This example is also analyzed by using ANSYS. The % difference of the dimen-

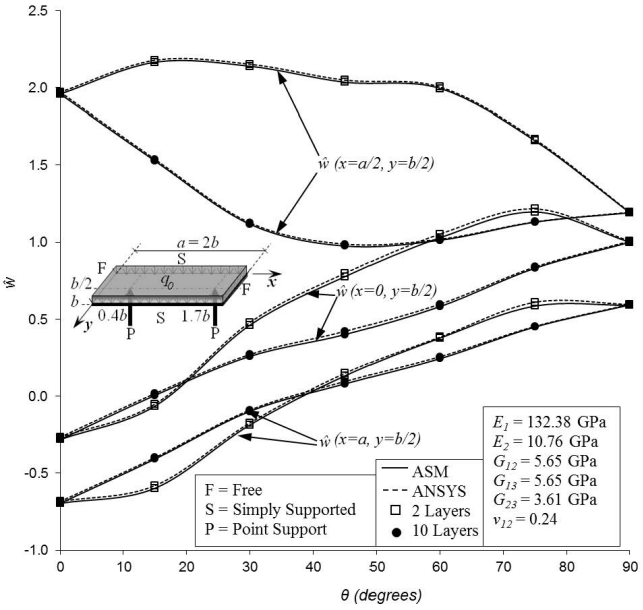

Figure 6: Dimensionless deflection $\hat{w} = \left(\frac{100E_2h^3}{b^4q}\right) w$ versus ply orientation angle, θ, at a uniformly loaded antisymmetric angle-ply rectangular laminated plate $(a/b = 2)$ having two internal point supports at $x = 0.4b$, $y = b/2$ and $x = 1.7b$, $y = b/2$.

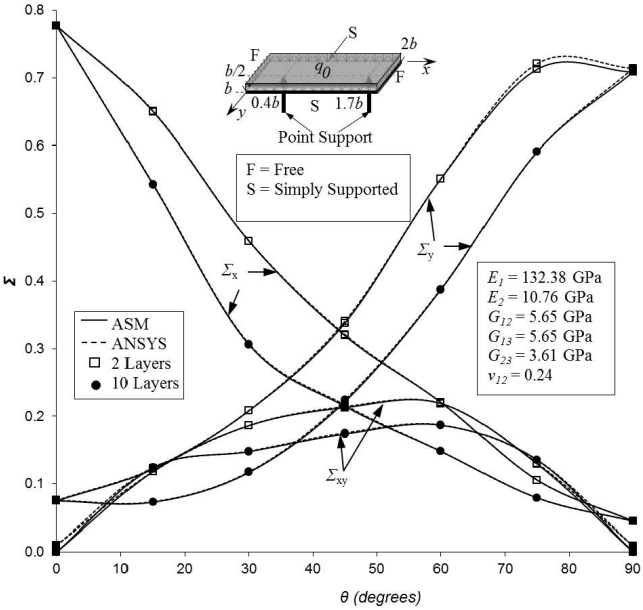

Figure 7: Dimensionless stresses, $\Sigma\left(\frac{a}{2}, \frac{b}{2}\right) = \left(\frac{h^2}{b^2q}\right)\sigma$, versus ply orientation angle, θ, for a uniformly loaded antisymmetric angle-ply rectangular laminated plate $(a/b = 2)$ having two internal point supports at $x = 0.4b$, $y = b/2$ and $x = 1.7b$, $y = b/2$, and simply supported at $y = 0$ and $y = a$.

sionless deflections $\left(100\frac{\hat{w}_{ANSYS} - \hat{w}_{ASM}}{\hat{w}_{ASM}}\right)$ is 0.21% at $x = 0$ and $y = a/2$, 0.99% at the center of the patch load, 0.52% at the center span of the intermediate beam sup-

port ($x = 7a/16$, $y = b/2$), and 1.24% at $x = a$ and $y = 3a/4$. The % differences for the dimensionless stresses $\left(100\frac{\Sigma_{ANSYS}-\Sigma_{ASM}}{\Sigma_{ASM}}\right)$ for Σ_x, Σ_y, and Σ_{xy} were less than 3%.

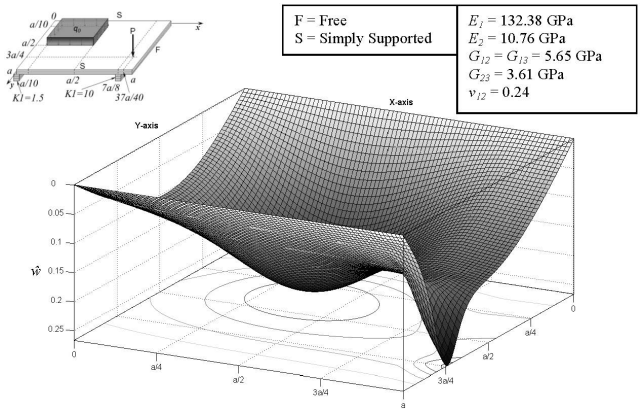

Figure 8: Contour of the dimensionless deflection for an antisymmetric angle-ply 6-layer (-15/-45/-75/75/45/15) square laminated plate simply supported at $y = 0$ and $y = a$, beam supported at $x = 0$ and at $x = 7a/8$, and subjected to a patch load and a concentrated load (Note: the isotropic beams are concentric and only half of the beams on bottom side of the plate are shown for clarity).

6 Summary and conclusions

The analytical Strip method (ASM) is extended in this paper to the analysis of stiffened and continuous antisymmetric laminated composite plates. The ASM can be used to analyze stiffened and continuous plates subjected to any combination of patch, uniform, line, and concentrated loads. Since results for stiffened and continuous antisymmetric laminates are not available in the literature, the results derived using the ASM are compared with ones derived using ANSYS, and they compare very well. The ASM solution overcomes the limitations of existing analytical methods and provides an alternative to numerical, semi-numerical, and approximate methods.

References

[1] Biswal K.C., Ghosh A.K., Finite element analysis for stiffened laminated plates using higher order shear deformation theory, Computers & Structures, 1994, 53(1), 161-171.

[2] Kolli M., Chandrashekhara K., Finite element analysis of stiffened laminated plates under transverse loading, Composites Science and Technology, 1996, 56(12), 1355-1361.

[3] Kumar Y.V.S., Mukhopadhyay M., A new triangular stiffened plate element for laminate analysis, Composites Science and Technology, 2000, 60(6), 935-943.

[4] Barik M., Mukhopadhyay M., A new stiffened plate element for the analysis of arbitrary plates, Thin-Walled Structures, 2002, 40 (7-8), 625-639.

[5] Harik I.E., Guo M., Ren W.X., Bending analysis of stiffened laminated plates, Advances in Structural Engineering, 2002, 5(3), 153-163.

[6] Li L., Ren X., Stiffened plate bending analysis in terms of refined triangular laminated plate element, Composite Structures, 2010, 92(12), 2936-2945.

[7] Thinh T.I., Quoc T.H., Finite element modeling and experimental study on bending and vibration of laminated stiffened glass fiber/polyester composite plates, Computational Materials Science, 2010, 49(4), Supplement, S383-S389.

[8] Bhar A., Phoenix S.S., Satsangi S.K., Finite element analysis of laminated composite stiffened plates using FSDT and HSDT: A comparative perspective, Composite Structures, 2010, 92(2), 312-321.

[9] Li D.H., Liu Y., Zhang X., Low-velocity impact responses of the stiffened composite laminated plates based on the progressive failure model and the layerwise/solid-elements method, Composite Structures, 2014, 110, 249-275.

[10] Hariri H., Bernard Y., Razek A., A two dimensions modeling of non-collocated piezoelectric patches bonded on thin structure, Curved and Layer. Struct., 2015, 2, 15–27.

[11] Natarajan S., Ferreira A.J.M., Nguyen-Xuan H., Analysis of cross-ply laminated plates using isogeometric analysis and unified formulation, Curved and Layer. Struct., 2014, 1, 1-10.

[12] Mukherjee A., Menghani L.C., Displacement and stress response of laminated beams and stiffened plates using a high-order element, Composite Structures, 1994, 28(1), 93-111.

[13] Sadek E.A., Tawfik S.A., A finite element model for the analysis of stiffened laminated plates, Computers & Structures, 2000, 75(4), 369-383.

[14] Qing G., Qiu J., Liu Y., Free vibration analysis of stiffened laminated plates, International Journal of Solids and Structures, 2006, 43(6), 1357-1371.

[15] Hadjiloizi D.A., Kalamkarov A.L., Metti, Ch., Georgiades A.V., Analysis of smart piezo-magneto-thermo-elastic composite and reinforced plates: Part I – model development, Curved and Layer. Struct., 2014, 1, 11–31.

[16] Hadjiloizi D.A., Kalamkarov A.L., Metti, Ch., Georgiades A.V., Analysis of smart piezo-magneto-thermo-elastic composite and reinforced plates: Part II – applications, Curved and Layer. Struct., 2014, 1, 32–58.

[17] Harik I.E., Bending of transversally loaded orthotropic rectangular and sector plates, Thesis submitted to Wayne State University, Detroit, Mich., in partial fulfillment of the requirement for the degree of Doctor of Philosophy, 1982.

[18] Harik I.E., Salamoun G.L., Analytical strip solution to rectangular plates, Journal of Engineering Mechanics, 1986, 112(1), 105-118.

[19] Harik I.E., Salamoun G.L., The analytical strip method of solution for stiffened rectangular plates, Computers & Structures, 1988, 29(2), 283-291.

[20] Sun L., Harik I.E., Application of the analytical strip method to antisymmetric laminates, ASCE Journal of Engineering Mechanics, 2010, 136(10), 1293-1298.

[21] Kong, J. and Cheung, Y.K., Application of the spline finite strip to the analysis of shear-deformable plates, Computers and Structures, 1993, 46(6), 985-988.
[22] ANSYS, Inc., Documentation for ANSYS, Revision 11.0, Canonsburg, PA, USA, 2007.
[23] Whitney J.M., Leissa A.W., Analysis of heterogeneous anisotropic plates, ASME Journal of the Applied Mechanics, 1969, 36(2), 261–266.
[24] Sharma S., Iyengar N.G.R., Murthy PN. Buckling of antisymmetric cross- and angle-ply laminated plates, International Journal of Mechanical Sciences, 1980, 22(10), 607-620.
[25] Reddy J.N., Mechanics of laminated composite plates and shells, Theory and Analysis, 2^{nd} Ed., CRC Press LLC, New York, 2004.
[26] Salamoun G.L., Harik I.E., Analytical strip solution for stiffened and continuous orthotropic rectangular plates, Report No. UKCE8503, Department of Civil Engineering, University of Kentucky, Lexington, KY, 1985.
[27] Editing Group of the Manual of Mathematics, Roots for quartic equation, Manual of mathematics, People's Education Press, Beijing, China, (Chinese), 1979, 87-90.
[28] Sun, L., Analytical strip method to antisymmetric laminated plates, Ph. D. Dissertation, University of Kentucky, Lexington, KY, 2009.